

See discussions, stats, and author profiles for this publication at: <https://www.researchgate.net/publication/262181150>

Understanding Molecular Interactions of Asphaltenes in Organic Solvents Using a Surface Force Apparatus

ARTICLE in THE JOURNAL OF PHYSICAL CHEMISTRY · JULY 2011

Impact Factor: 2.78 · DOI: 10.1021/jp2039674

CITATIONS

21

READS

63

7 AUTHORS, INCLUDING:



Shengqun Wang

University of Alberta

8 PUBLICATIONS 169 CITATIONS

[SEE PROFILE](#)



Qingxia Liu

University of Alberta

78 PUBLICATIONS 792 CITATIONS

[SEE PROFILE](#)



Hongbo Zeng

University of Alberta

135 PUBLICATIONS 1,950 CITATIONS

[SEE PROFILE](#)



Zhenghe Xu

University of Alberta

335 PUBLICATIONS 7,043 CITATIONS

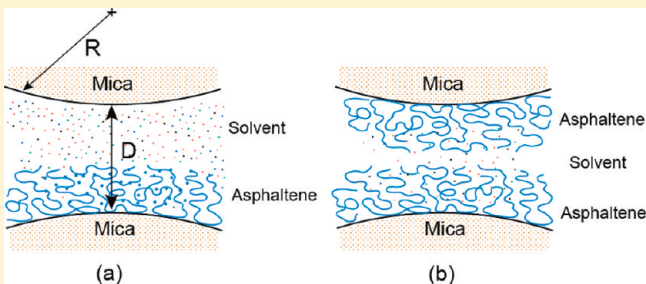
[SEE PROFILE](#)

Understanding Molecular Interactions of Asphaltenes in Organic Solvents Using a Surface Force Apparatus

Anand Natarajan,[†] Jinggang Xie,[†] Shengqun Wang, Qingxia Liu, Jacob Masliyah, Hongbo Zeng,* and Zhenghe Xu*

Department of Chemical and Materials Engineering, University of Alberta, Edmonton, Alberta, T6G 2 V4, Canada

ABSTRACT: A surface force apparatus was used to study the intermolecular forces of asphaltenes in toluene and heptane. The repulsive interaction forces measured between two asphaltene surfaces in toluene were shown to have a steric nature and could be described by the Alexander–de Gennes theory on steric repulsion between two interacting polymer layers in good solvents at short separation distances under high compression forces. On the other hand, the adhesion forces measured between asphaltenes in heptane can be described by van der Waals forces, which are responsible for asphaltene aggregation and precipitation in paraffinic solvents. The asphaltene films adsorbed on mica were found to swell significantly in toluene but only moderately in heptane. In addition, an adhesion force was observed between an asphaltene surface and a mica surface in toluene. The results from this study provide an insight into the basic interaction mechanisms of asphaltenes in organic media and hence in crude oil and bitumen production.



INTRODUCTION

Asphaltenes are normally defined as the part of the crude that is soluble in toluene and insoluble in alkanes, usually *n*-pentane or *n*-heptane.^{1,2} The above definition indicates that asphaltenes do not comprise a chemically defined group of molecules but rather a solubility class. In general, asphaltene molecules are large polyaromatic hydrocarbons containing a significant number of heteroatom functional groups including both acids and bases.³ The functional groups are typically hydrophilic, while the hydrocarbon structure of asphaltenes is hydrophobic. Hence, asphaltenes are considered surface active and are able to adsorb at water–oil interfaces. The adsorbed asphaltenes, together with the accumulation of other surface active materials such as resins, natural surfactants and fine solids, form a protective interfacial film that prevents the dispersed water droplets from coalescence, thereby stabilizing water-in-oil (w/o) emulsions.^{4–17} Stable emulsions are undesirable in petroleum processing because the presence of w/o emulsions leads to serious processing problems in downstream operations, e.g. corrosion, erosion, and fouling in the heat exchangers, transportation device, and distillation equipment, causing a significant increase in operating cost. Despite the extensive research reported on w/o emulsions, the exact stabilization mechanism remains to be established. Many believe that asphaltenes are almost exclusively responsible for stabilizing w/o emulsions,^{18–20} while others believe that only a small fraction of total asphaltenes is involved in stabilization of w/o emulsions.^{21,22} Many other industrial problems such as wellbore or pipeline plugging, alteration of wettability of solids, and sedimentation during crude blending are all attributed, at least partly, to molecular aggregation of asphaltenes upon exposure to an unfavorable liquid environment, to an oil–water interface or to various solid–oil

interfaces. Thus, understanding the role of asphaltenes in stabilization of w/o emulsions at the molecular level is of both fundamental and practical importance.

The behavior of asphaltenes in a crude oil is almost exclusively determined by interactions between asphaltene molecules/aggregates in the surrounding organic solvents. Significant efforts have been made during the past decade in this regard. Several microscopic and nanoscopic techniques, including micropipette and Langmuir trough have been used to study molecular interactions of asphaltenes and its relation to stability of w/o emulsions. The micropipette technique allows micrometer-size emulsion droplets to attach onto a small pipette, which has been used to study water-diluted bitumen interfacial properties such as interfacial tension, crumpling ratio, and interfacial rheology.^{23,24} A Langmuir trough was used to measure surface pressures of asphaltene layers formed at the water–toluene interface.^{25–27} The Langmuir trough results showed that the asphaltene layer is rigid and irreversibly adsorbed at the water–toluene interface, which accounts for the observed difficulties to disrupt the protective asphaltene layers surrounding the emulsified water droplets in diluted bitumen.

Surface forces between asphaltene surfaces in aqueous solutions have been measured directly using an atomic force microscope, as were a number of quantitative studies conducted on colloidal force measurements between solids and model oil droplets.^{28–31} Reports on surface forces for crude oil systems in aqueous solutions are also available.^{4,32–35} To understand the colloidal interactions between oil sand components in aqueous

Received: April 28, 2011

Revised: June 5, 2011

Published: July 27, 2011

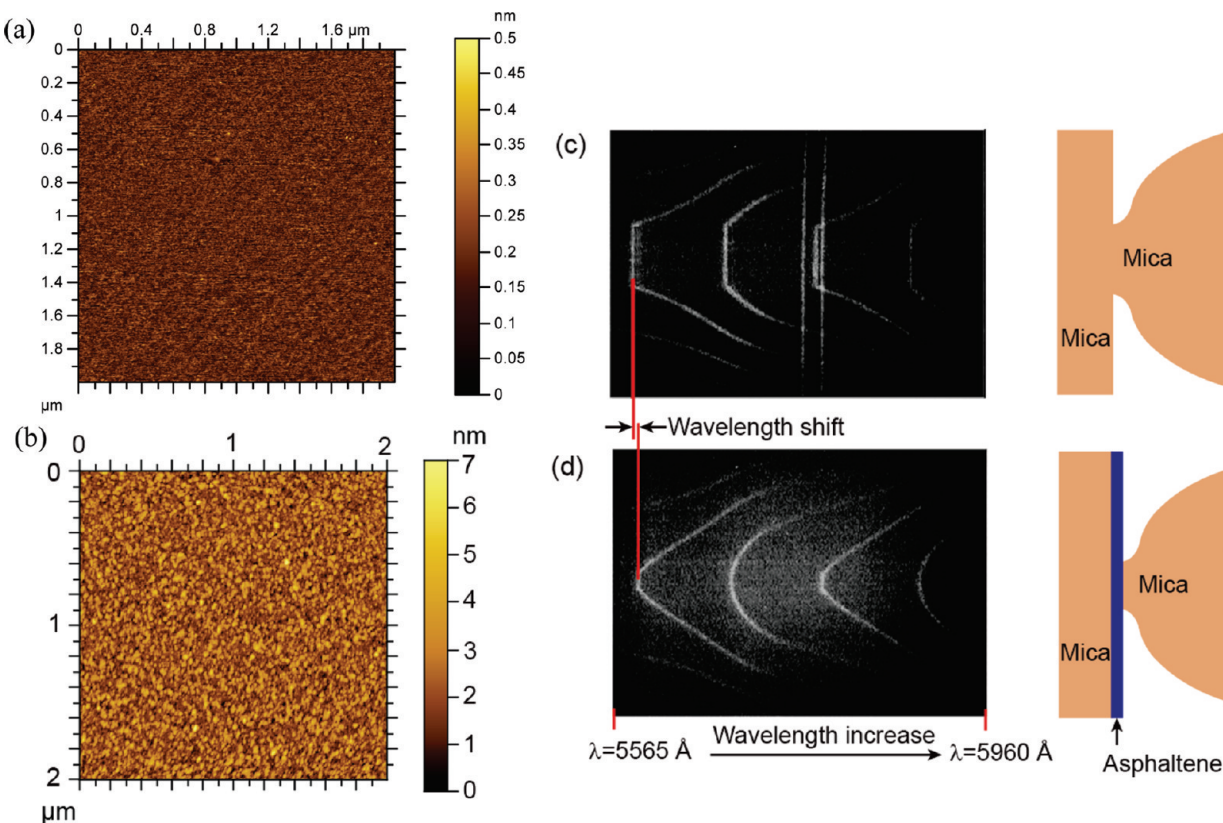


Figure 1. AFM images of (a) bare mica surface and (b) coated asphaltene film on mica surface. (c) FECO of mica surfaces in contact in air. (d) FECO of a coated asphaltene film in contact with a mica surface in air. Note the shift in the wavelength of FECO and change in the shape (contact area) of the fringes, indicating the presence of asphaltene layers and change of adhesion due to the presence of asphaltenes as anticipated. FECO can be used to measure surface deformation, separation distance between two surfaces and refractive index of the medium.

solutions, a number of systematic studies were conducted using atomic force microscopy (AFM) to measure surface forces between bitumen and silica,³⁶ bitumen and clay,³⁷ bitumen and fine solids,³⁸ bitumen and bitumen,³⁹ silica and clay,⁴⁰ and asphaltenes and asphaltenes.⁴¹ These studies provided a better understanding of and scientific guidance to bitumen extraction and flotation during oil sand processing. Although there are many reports on direct surface force measurements in aqueous systems using AFM or surface force apparatus (SFA), less attention has been devoted to nonaqueous systems. Recently, Wang et al. reported measurements of interaction forces between asphaltene films or asphaltene films and a micrometer-sized silica sphere in oil media using an AFM,^{42,43} while Vuillaume et al. used a SFA to measure interaction forces between mica surfaces across asphaltene solutions and crude oil in the presence and absence of water.⁴⁴ These measurements provided valuable information on stabilization mechanism of the water-in-diluted bitumen emulsions as of steric origin. Because of the complexity of the water-in-diluted bitumen emulsion systems and limitations of techniques described above, understanding of interfacial properties, intermolecular and surface interactions of asphaltenes, and corresponding governing mechanisms on the stability of water-in-oil emulsions remains incomplete.

In the present study, we focus on understanding the interactions of two asphaltene films in good/poor solvents (toluene and heptane). Because of its unique ability to measure simultaneously the interaction force, F , as a function of the absolute surface separation, D , and the local geometry of two interacting surfaces (the local radius R or contact area) at a force sensitivity of ~ 10 nN

and an absolute distance resolution of 0.1 nm *in situ* and in real time, SFA has been widely used in studying governing forces of many biological and nonbiological systems.⁴⁵ SFA could be a unique and ideal technique for the research objective of this study. The force-distance curves or so-called force profiles obtained from SFA measurements would be able to provide valuable information on material properties such as interaction energies, Hamaker constant, and molecular conformation changes of the interacting asphaltene surfaces or films in a given solvent. AFM imaging was employed to provide complementary information on the surface morphology of the asphaltene films studied.

MATERIALS AND EXPERIMENTAL METHODS

Materials. Vacuum distillation feed bitumen was provided by Syncrude Canada Ltd., Alberta, Canada. Asphaltenes were precipitated from bitumen by adding 40 times of *n*-heptane to bitumen by volume and repeatedly washing with *n*-heptane. Details on asphaltene precipitation were reported elsewhere.¹⁴ High-performance liquid chromatography (HPLC)-grade toluene and heptane purchased from Fisher Scientific were used as received. Ruby mica sheets were purchased from S & J Trading Inc. (Glen Oaks, NY).

Sample Preparation. A film-coating method was adopted to coat an asphaltene film on a mica surface. Briefly, after gluing a freshly cleaved thin mica sheet on a silica disk used as support, several drops of 0.5 wt % asphaltene in toluene solution were placed and spread on the exposed mica surface. The solvent was

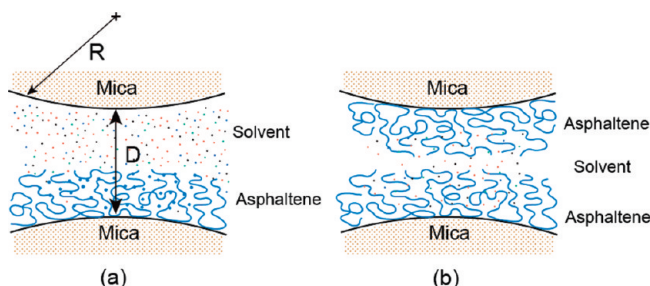


Figure 2. Experimental configurations for studying the surface interactions of asphaltenes in organic solvents: (a) an asphaltene film vs a bare mica (asymmetric case) and (b) two asphaltene films (symmetric case).

evaporated for ~ 15 min to immobilize asphaltenes on the mica surface. The sample was then washed with pure toluene and blow-dried with ultrapure nitrogen before it is loaded in the SFA chamber. The asphaltene-coated mica surfaces were then used to measure interaction forces and image their topographic features by SFA and AFM, respectively.

Surface Force Apparatus Technique. A surface force apparatus (Surforce LLC, Santa Barbara, CA, USA) was used to measure the normal interaction forces between two asphaltene films immobilized on mica in organic solvents. A detailed setup of SFA experiments has been reported elsewhere.^{45,46} Briefly, the back surface of a thin mica sheet ($1\text{--}5 \mu\text{m}$ thick) was coated with an ~ 50 nm thick semi reflective layer of silver, required to obtain multiple beam interference fringes of equal chromatic order (FECO). The FECO was used to determine the surface separation, surface geometry and deformation, and the contact area *in situ* and in real time. The silver-coated mica sheet was glued using glucose onto a cylindrical silica disk (radius $R = 2$ cm). The prepared silica disks were then mounted into the SFA chamber in a cross-cylinder geometry, which roughly corresponds to a sphere of radius R approaching a flat surface locally. With this arrangement, the measured force $F(D)$ is converted to interaction energy per unit area between two flat surfaces, $W(D)$ using the Derjaguin approximation:^{46,47} $F(D) = 2\pi R W(D)$. In each set of measurements, the reference distance ($D = 0$) was determined at the adhesive contact between the two bare mica surfaces in air prior to introducing the solvents between the surfaces. For the force measurements, $\sim 50 \mu\text{L}$ of desired solvent/solution was injected between two closely placed mica surfaces with or without coated asphaltenes in the SFA chamber. The chamber was sealed and saturated with the vapor of the same solvent. Normal forces between the two surfaces were measured by moving the lower surface supported on a double-cantilever “force springs” toward the upper surface by a distance $\Delta D_{\text{applied}}$. The actual distance that the surfaces moved to each other, ΔD_{meas} , was measured by multiple beam interferometry in real time.⁴⁸ The change in the force ΔF between the surfaces, when they come to rest at a separation distance D , was calculated from the deflection of the cantilever spring by $\Delta F(D) = k(\Delta D_{\text{applied}} - \Delta D_{\text{meas}})$, where k is the spring constant. When $\partial F(D)/\partial D > k$, there is a mechanical instability that causes the lower surface to jump either toward or away from the upper surface during approaching or separation process, respectively. During a typical force measurement, the normal force–distance (F vs D) profile was obtained by an initial approach to a “hard wall” followed by separation of the two surfaces (note the “hard wall” distance in this study is defined as the mica–mica separation distance or thickness of confined asphaltenes which barely changed with increasing the normal load or pressure).

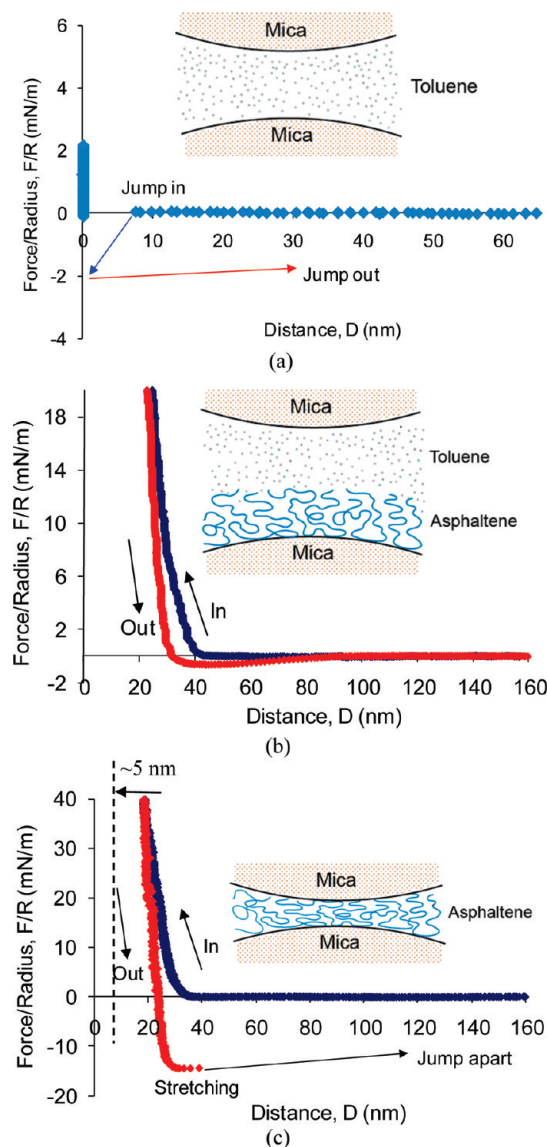


Figure 3. Force profiles of a coated asphaltene film on surface interacting with a bare mica surface across toluene: (a) two bare mica surfaces in pure toluene, (b) measurement after the asphaltene film being exposed in toluene for ~ 1 h, and (c) successive measurement in which the asphaltene film was kept in contact with mica surface for about 10 min before separation. When the surfaces are compressed, the hard wall shifted to about 5 nm indicating that asphaltene film in toluene swell and is flexible instead of rigid. In this figure and all subsequent figures, “In” indicates approach of the two surfaces and “Out” indicates separation of the two surfaces.

RESULTS AND DISCUSSION

The topographical features of asphaltene films immobilized on mica surfaces were imaged in air by an AFM operating in tapping mode. As shown in Figure 1a, the AFM image of bare mica prior to asphaltene film deposition showed a featureless and molecularly smooth surface with a root-mean-square (rms) roughness of 0.3 nm. The AFM image of coated asphaltene film on mica in Figure 1b shows a rms roughness of 0.9 nm. Typical FECO fringe of two mica surfaces in contact in air is shown in Figure 1c and FECO of an asphaltene film in contact with mica in air is shown in Figure 1d. Taking the distance of two mica surfaces as zero, the

thickness of an asphaltene film in air was determined to be ~ 5 nm. The intermolecular forces of asphaltenes immobilized on mica in organic solvents were measured using an SFA in two different configurations as shown in Figure 2. Figure 2a shows an asymmetric geometry of an asphaltene film coated on mica interacting with a bare mica surface in a solvent. Figure 2b shows a symmetric geometry of two asphaltene films coated on mica in a solvent of interest.

Interaction Forces in Toluene (Good Solvent). Asphaltenes are soluble in toluene. To that end, toluene can be considered as a good solvent that significantly mediates the configuration of asphaltene molecules on a substrate and hence affects the interaction forces. In this study, the force profile of two bare mica surfaces in toluene was first determined. As shown in Figure 3a, an attractive interaction force was observed as the two mica surfaces approach each other. The two surfaces jumped at $D_J \approx 7.5$ nm into contact. When the surfaces were separated, a very strong adhesive force was observed and the surfaces jumped apart from contact. For two surfaces 1 and 2 in a geometry of two crossed cylinders having the same radius R approaching each other in a medium 3, the attractive van der Waals force is given by eq 1, and the critical jump-in distance D_J is given by eq 2

$$F_{vdW} = -\frac{A_{132}R}{6D^2} \quad (1)$$

$$D_J = \left(\frac{A_{132}R}{3k} \right)^{1/3} \quad (2)$$

where D is the distance between the two curved surfaces, k is the force-measuring spring constant, and A_{132} is the combined Hamaker constant of the two surfaces 1 and 2 interacting across 3.⁴⁹ A_{132} can be estimated using eq 3

$$A_{132} \approx (\sqrt{A_1} - \sqrt{A_3})(\sqrt{A_2} - \sqrt{A_3}) \quad (3)$$

where A_1 , A_2 , and A_3 are the Hamaker constants of media 1, 2, and 3 in vacuum. In this experiment, two bare mica surfaces (surface 1 = surface 2) approach each other in toluene (medium 3). With the measured values of $D_J \approx 7.5$ nm and $k \approx 500$ N/m, the Hamaker constant of $A_{\text{mica-toluene-mica}} = 3kD_J^3/R$ is estimated to be 3.2×10^{-20} J.

By use of the literature Hamaker constants of $A_{\text{mica}} \approx (15.8 \pm 2.5) \times 10^{-20}$ J and $A_{\text{toluene}} \approx 5.4 \times 10^{-20}$ J, eq 3 gives $A_{\text{mica-toluene-mica}} \approx ((A_{\text{mica}})^{1/2} - (A_{\text{toluene}})^{1/2})^2 \approx 2.7 \times 10^{-20}$ J.⁴⁶ This value is in agreement with the above experimentally measured value, validating the experimental setup and accurate measurement in organic solvents.

The interactions between a coated asphaltene film and a bare mica surface in toluene were measured. Figure 3b shows the interaction force measured after exposing asphaltenes to toluene for ~ 1 h. The two surfaces were brought into contact and then separated immediately. Repulsive force was observed during approach at around 40 nm with a hard wall distance of ~ 22 nm. A weak adhesive force ($F/R \approx -0.6$ mN/m) was observed during separation. On the next approach at the same position, shown in Figure 3c, a repulsive force was observed at about 5 nm closer than the previous approach, shown in Figure 3b, while the hard wall shifted to ~ 18 nm. After keeping the asphaltene film and mica surface in contact in toluene for ~ 10 min before separation, a much stronger adhesion force was measured ($F/R \approx -14.5$ mN/m). Under high compression of ~ 2 MPa, the hard wall separation shifted to ~ 5 nm, which

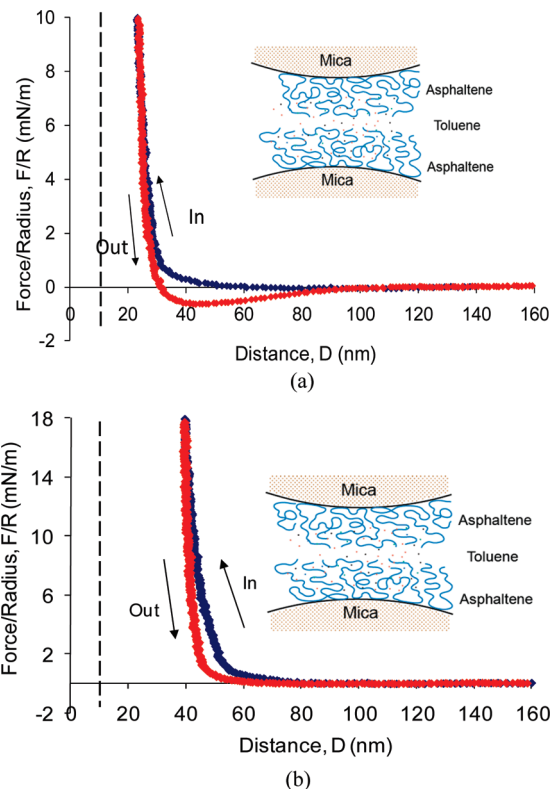


Figure 4. Force profiles of (a) asphaltene-coated surfaces in toluene immediately after toluene injection and (b) asphaltene-coated surfaces in toluene after 30 min. The vertical dashed lines indicate the hard wall distance of two asphaltene surfaces in air.

corresponds to the thickness of coated asphaltene film in air on the mica surface.

The force profiles for coated asphaltene films in toluene are shown in Figure 4a (measured immediately after toluene injection) and Figure 4b (measured ~ 30 min after toluene injection). Weak adhesion was measured during the separation for the initial measurement, which disappeared when measured after 30 min of incubation of the system. Interestingly, the hard wall distance in reference to mica–mica separation distance in toluene, i.e., the thickness of the confined asphaltenes in toluene shifted from ~ 25 to ~ 40 nm between the two measurements. However, when a higher load/pressure (~ 1 MPa) was applied, the confined asphaltene thickness decreased to ~ 11 nm, which corresponds to two asphaltene films ~ 5.5 nm thick on each mica surface. This finding suggests that asphaltene layers in toluene swelled in 30 min by 60%, i.e., up to about ~ 15 nm on each surface. Also, the swollen asphaltene layers are flexible and soft instead of being rigid.

Since the electric double-layer forces in toluene can be considered negligible, repulsive forces observed during the approaching of two asphaltene films in toluene as shown in parts a and b of Figure 4 are attributed to steric repulsion of swollen asphaltene chains.⁴² The retracting force profile in Figure 4a shows a weak adhesion, most likely due to the interdigitation and bridging of the asphaltene molecules on the two surfaces when brought in contact for a few seconds during force measurements. Such interactions resulted in stretching of the asphaltene layers up to $D \approx 40$ nm during separation before the two surfaces finally detached from each other. As shown in Figure 4b, this bridging

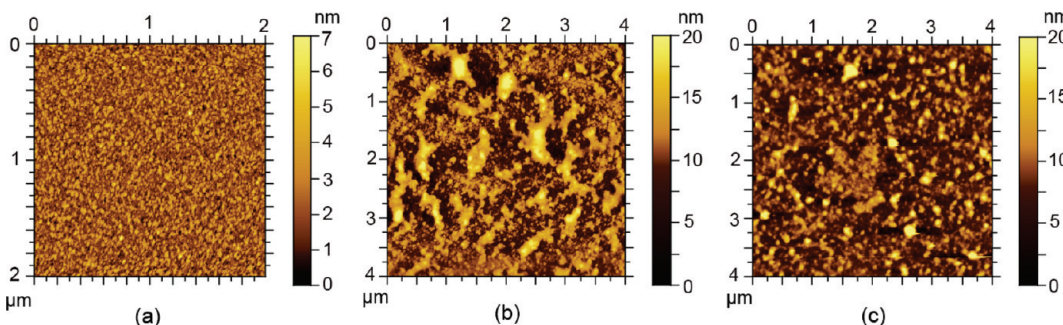


Figure 5. AFM image of asphaltene-coated on mica surfaces. (a) Coated asphaltene film on mica in air, (b) coated asphaltene film on mica after incubation in toluene for 30 min, showing significant aggregation, and (c) coated asphaltene film incubated in heptane for 30 min, showing less significant aggregation than in toluene.

adhesion force disappeared after 30 min incubation of asphaltene in toluene, accompanied by a much longer range repulsion. It appears that asphaltenes are fully solvated during this period in a good solvent, leading to the conformational change which was confirmed by the AFM images of coated asphaltene surfaces before and after immersion in toluene for 30 min as shown in parts a and b of Figure 5. The rms roughness of asphaltene surfaces increased from 0.9 to 2.8 nm, and the aggregates become much larger after immersion of asphaltene films in toluene for half hour. Such an increase in surface roughness by soaking asphaltene films in toluene leads to a greater hard wall distance as shown in Figure 4b. Since asphaltenes are amphiphilic and highly soluble in toluene, most of the polar functional groups stick to the mica surface with time, leaving the rest of the molecules being extended into toluene. In this manner, the side chains of asphaltene aggregates mimic a swollen brush and repel each other when brought in contact. This argument is supported by repulsive forces and ~ 15 nm surface shift of the hard wall distance as shown in parts a and b of Figure 4. The hard wall can be pushed to about ~ 11 nm under a compressive load/pressure of ~ 1 MPa, indicating that the asphaltene layers are soft and that they swell in toluene.

The force profile for the interaction between two mica surfaces immediately following the injection of 0.5 wt % asphaltene in toluene solution is shown in Figure 6a. The asphaltenes in the solution adsorbed very quickly (less than 5 min) to the mica surfaces, and the hard wall distance increased to ~ 30 nm. A weak adhesive force of $F/R \approx -1$ mN/m was observed during separation. The asphaltene–toluene solution was flushed out and replaced by pure HPLC toluene. The force profile in Figure 6b shows that only pure repulsive forces were observed with the hard wall distance shifted to ~ 40 nm. This result is similar to the interaction between two coated asphaltene films on mica in toluene as shown in Figure 4.

As toluene is a good solvent for asphaltenes, the side chains/branches of the immobilized asphaltene molecules on mica surface tend to stretch and act as a swollen brush while the aggregated core could swell to become mushroom-type conformations. Consequently, the adsorbed asphaltene film on mica may be treated as a polymer brush, and the interaction between two such films could be described by the Alexander–de Gennes (AdG) theory on two interacting polymer brush layers.^{50–53} When two polymer brush surfaces approach each other, at some distance the brushes/films start to overlap. The increased local density of polymer segments lead to an increase in osmotic pressure and repulsive interaction energy. The repulsive pressure

between two planar brush layers is given by⁵⁴

$$P(D) \approx \frac{kT}{s^3} \left[\left(\frac{2L}{D} \right)^{9/4} - \left(\frac{D}{2L} \right)^{3/4} \right] \text{ for } D < 2L \quad (4)$$

where s is the mean distance between anchoring (or grafting) sites on the surface, L is the brush layer thickness per surface, T is the temperature, and k is Boltzmann constant. For the geometry of two crossed cylinders of radius R (used in our SFA measurements), the force between them is given by first integrating the above equation and then using the Derjaguin approximation as^{46,54}

$$\begin{aligned} \frac{F(D)}{R} &= 2\pi \int P(D)dD \\ &= \frac{16\pi kTL}{35s^3} \left[7\left(\frac{2L}{D}\right)^{5/4} + 5\left(\frac{D}{2L}\right)^{7/4} - 12 \right] \end{aligned} \quad (5)$$

For the asymmetric case (a brush layer against a solid substrate), the equation becomes

$$\frac{F(D)}{R} = \frac{8\pi kTL}{35s^3} \left[7\left(\frac{L}{D}\right)^{5/4} + 5\left(\frac{D}{L}\right)^{7/4} - 12 \right] \quad (6)$$

The fit of measured repulsive forces for two asphaltene films in toluene with the AdG theory (eqs 5 and 6, solid curves) is shown in Figure 7a, while for asphaltene film interacting with a mica surface in Figure 7b. As shown in Figure 7a, the AdG model fits the measured force profile well at short separation distances under high compression forces. However, a significant deviation is seen at longer separation distances under lower compression forces. It appears that the protrusion or undulation of aliphatic side chains on asphaltene brushes and aggregates in good solvent induces a weaker repulsive force over a much longer separation distance. This additional force is not considered in the AdG theory applicable to monodisperse brushes. In fact, lower compression regime can be fitted with the AdG theory using an independent set of parameters as shown in Figure 7a, indicating the presence of possible secondary brushes in the current systems due to the polydispersity/complexity of asphaltene molecules/aggregates. It is interesting to note that such deviation is not visible in Figure 7b for asymmetrical cases, possibly due to longer incubation time and/or limited sensitivity of single asphaltene layer. From the fitted parameters of s and L listed in Table 1, it is interesting to note that for both the symmetric and asymmetric cases, the fitted mean distance between anchoring (or grafting) sites s are very close to each other as anticipated and also close to

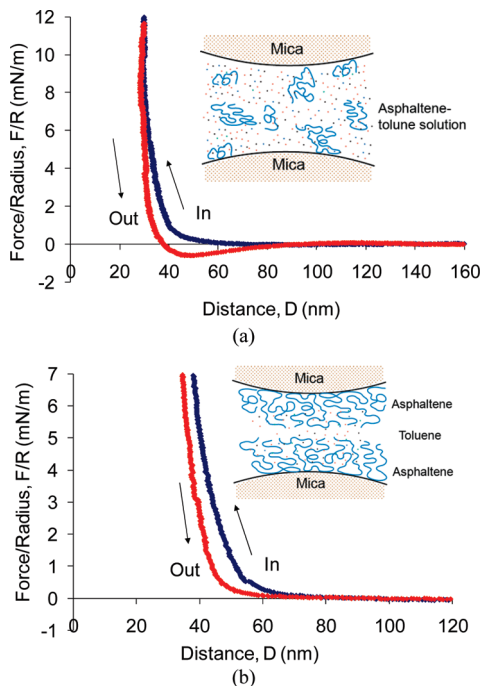


Figure 6. Force profiles of (a) mica surfaces in asphaltene–toluene solution measured immediately after injection. (b) Same system as (a) but after the asphaltene–toluene solution is flushed out and replaced by pure toluene and measured after 30 min.

the size of nanoaggregates of asphaltenes in bulk toluene solutions.⁵⁵ The thickness of brush layer L depends on compression pressure and immersion time in toluene, which causes aggregation and swelling of asphaltene molecules and aggregates. This observation is consistent with surface morphological features revealed in AFM images shown in Figure 4. It is interesting to note that regardless of the swollen thickness in either symmetrical or asymmetrical cases, the final thickness of each asphaltene film after high pressure compression is the same of ~ 5 nm as anticipated.

Interaction Forces in Heptane (Poor Solvent). Heptane is a paraffinic and apolar organic solvent, while asphaltene molecules are highly aromatic with a significant number of heteroatoms. Therefore asphaltene and heptane are very different in their molecular structure. Heptane is known to be a poor solvent for polyaromatic asphaltenes. In heptane asphaltenes tend to self-aggregate and precipitate, which is very different from their state in toluene. The interaction force profile between two coated asphaltene films in heptane is shown in Figure 8. The effective Hamaker constant of two asphaltene films across a liquid heptane, $A_{\text{asphaltene-heptane-asphaltene}}$ is 1.1×10^{-21} J.^{43,46,56,57} With the spring stiffness used for this experiment $k \approx 880$ N/m, eq 2 predicts a jump-in distance $D_j = (A_{\text{asphaltene-heptane-asphaltene}} R / 3k)^{1/3} \approx 2$ nm for two smooth asphaltene films in heptane. However, no jump-in was observed during the approach of the two asphaltene films. Using AFM, Wang et al.⁴³ observed a weak attractive force when two asphaltene surfaces approach each other in heptane. The difference in our results is attributed to surface roughness resulted from self-association of asphaltene molecules, as observed in the AFM image shown in Figure 5c, and also the strong spring constant that was used in the SFA experiments. Strong adhesion force of $F/R \approx -3$ mN/m was however measured during the separation as shown in Figure 8a.

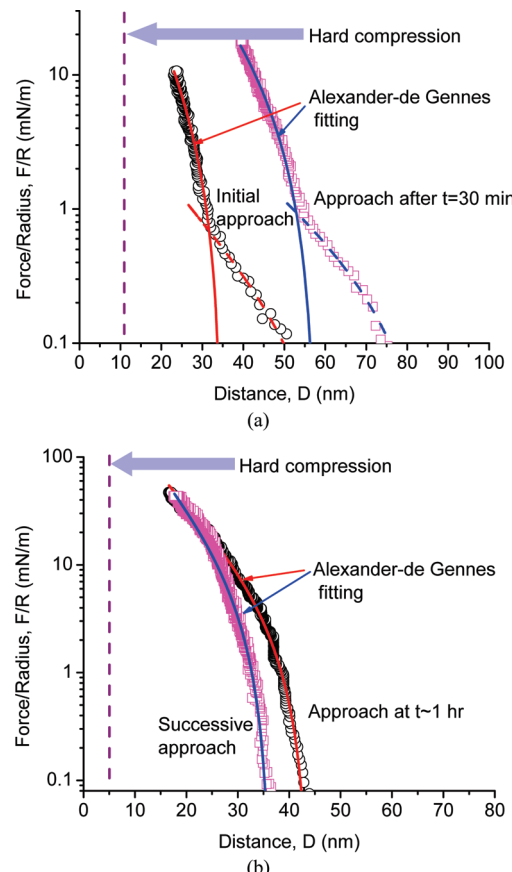


Figure 7. Experimentally measured repulsion forces and best fitted curves using the AdG theory for approach of (a) two asphaltene films and (b) an asphaltene film against a bare mica surface in toluene.

The force profile of separation indicates a significant stretch of asphaltene films by ~ 10 nm before the two surfaces detached from each other. Similar force profile was measured after 30 min immersion in heptane, as shown in Figure 8b, although a weaker adhesion of $F/R \approx -1$ mN/m and a slightly larger hard wall distance of ~ 20.5 nm were determined, in comparison to ~ 16.5 nm observed at initial approach shown in Figure 8a.

The adhesion forces measured between two asphaltene films in heptane are attributed to the van der Waals interactions,^{58,59} which are stronger than that in toluene. The current study demonstrates that van der Waals forces are responsible for asphaltene flocculation in paraffinic solvents. By comparison of Figures 4 and 8, one can observe clearly that the hard wall shift after 30 min immersion in solvent is greater for two asphaltene films in toluene (Figure 4b) than in heptane (Figure 8b). The hard wall distance in the heptane system is ~ 20 nm shorter, suggesting a much less significant swelling of asphaltene molecules in heptane than in toluene. Nevertheless, a small hard wall shift of ~ 4 nm in heptane does indicate some morphology changes of the asphaltene films (limited swelling or molecular rearrangement) upon exposure to heptane. The AFM image of the asphaltene films immersed in heptane for half hour in Figure 5c shows many smaller asphaltene aggregates as compared with the initial smooth surface shown in Figure 5a. The results from both SFA force measurement and AFM imaging suggest that certain fractions of asphaltenes are able to have

Table 1. Fitting Parameters Using the AdG Scaling Theory

asphaltene surfaces in toluene			
~5 min of immersion		~35 min of immersion	
L (nm)	high loading ^a	low loading ^b	high loading
s (nm)	2.8	12.5	2.7
			10.0

asphaltene and mica surfaces in toluene	
~60 min of immersion	
L (nm)	44.0
S (nm)	3.2
	37.0
	2.5

^a High compression and short separation distance regime (solid fitting curve in Figure 7a). ^b Low compression and long separation distance regime (dash fitting curve in Figure 7a).

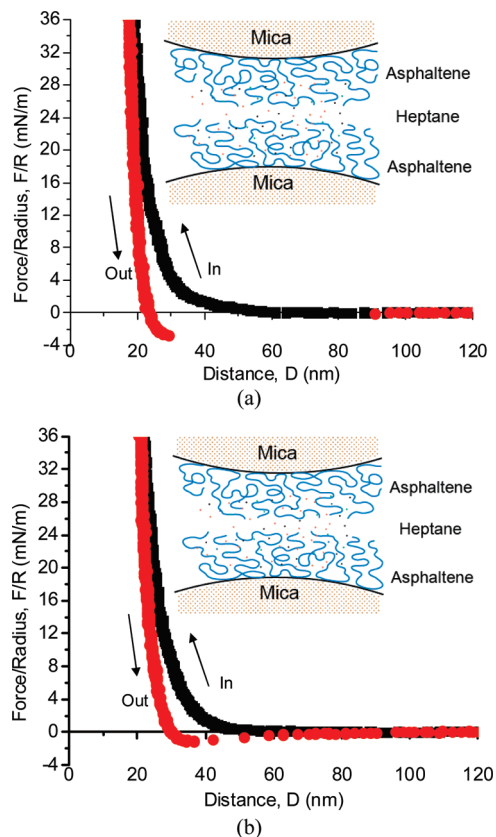


Figure 8. Force profiles of two asphaltene films in heptane. (a) Force–distance curves measured immediately after heptane injection and (b) force–distance curves measured after ~30 min immersion in heptane.

limited swelling in heptane, resulting in rearrangement and aggregation of these fractions of asphaltene molecules to minimize the total energy in the heptane system. The interactions between an asphaltene film and a bare mica surface in heptane were also studied, and similar force profiles and adhesion forces were obtained as in asymmetrical toluene systems.

Stability of w/o Emulsions. w/o emulsions are highly undesirable in petroleum processes as they lead to serious processing

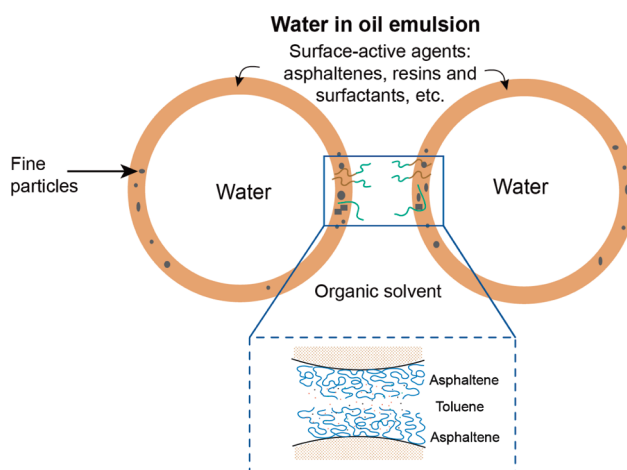


Figure 9. Schematic illustration of a rigid interfacial film formed by asphaltenes, resins, fine particles, etc., adsorbed at the water–oil interface, preventing water droplets from coalescing and thereby stabilizing the water-in-oil emulsions, which is highly undesirable in petroleum processes.

problems such as equipment fouling and corrosion and cause significant cost increase because of transportation difficulties and equipment corrosion. The stability of w/o emulsions is directly related to the water–oil interfacial properties.

Strong repulsive force or the absence of adhesion between emulsified droplets usually corresponds to higher emulsion stability, while a weaker repulsion or a strong adhesion can lead to flocculation and instability of emulsions. The SFA measurements in this study show that asphaltene surfaces swell significantly in toluene, leading to strong steric repulsion. In contrast, asphaltenes show a strong adhesion between asphaltene and hydrophilic mica surfaces in toluene, providing an attractive force between the two surfaces. These findings suggest that fine hydrophilic solid/clay particles are able to aggregate with the asphaltene residues and with each other in toluene. Since asphaltenes are known to be amphiphilic, the asphaltene and fine particle aggregates would prefer to stay at the water–oil interface and form a semirigid interfacial film. The presence of such rigid interfacial films and strong steric repulsion between two asphaltene surfaces lead to a strong energy barrier preventing the water droplets from attaching to each other and coalescing. This is the case of commercial process for the naphtha-based bitumen froth treatment (cleaning) process in the oil sand industry. Because naphtha is a mixture of aromatic and aliphatic/naphthenic hydrocarbons, which is a relatively good solvent for asphaltenes (no asphaltene precipitation occurs at the industrial dilution ratio), 1–2 wt % residual emulsified water droplets are always present in the final diluted bitumen product. In this study we used the asphaltene films on the mica surface to mimic the stable interfacial film and the mica surfaces to mimic the clay surfaces as shown in Figure 9. Such an approach has been used in a number of previous studies where a solid substrate supported polymer or surfactants layer was used to mimic the interface between two fluidlike phases/domains.^{41,44,60–64} The results of this study provide an insight into the intermolecular interactions of asphaltene–asphaltene and asphaltene–clay surfaces in organic media of varying solvent quality. To fully understand the stability of water-in-oil emulsions as encountered in heavy oil processing; however, other factors such as naphthenic acid, resins, and moisture/water content need to be included. To break this stable w/o emulsion, demulsifiers

are needed to eliminate the repulsive forces by destroying the asphaltene films adsorbed on the water surface. This part of discussion will be illustrated in a subsequent paper.

CONCLUSION

The forces between coated asphaltene films in toluene and heptane were measured using a SFA. The SFA force measurements allowed a direct evaluation on molecular interactions of asphaltenes in organic solvents, providing insight of molecular aggregation, rearrangements, and swelling of asphaltenes in toluene and heptane. AFM was used to obtain complementary information on the morphology change of the asphaltene films in organic solvents with time. The results of this study show that the surface interactions of asphaltenes strongly depend on the type of solvent, contact time, and load (pressure) applied to the asphaltene films during the force measurement. Adhesion forces were measured between asphaltene and mica in both toluene and heptane as well as between two asphaltene films in heptane. Although small adhesion was initially observed for two asphaltene films in toluene, pure repulsion was observed with increasing film incubation time, which was attributed to steric repulsion of swollen asphaltene films. The steric repulsion at short separation distances under high compression forces fits well with the AdG scaling theory of two interacting polymer brush layers. The deviation of steric repulsion at large separation distances under lower compression forces from the AdG scaling theory suggests the presence of secondary structures of asphaltenes in good solvent, most likely stemming from the polydispersity/complexity of asphaltene molecules/aggregates. The AFM experiments showed significant changes with time, in conformation and morphology of asphaltene films in toluene, which were less significant in heptane, accounting for the observed results from the SFA force measurements. The steric repulsion between asphaltene films in toluene and adhesion force between asphaltene and mica surfaces contribute significantly to the stability of the water-in-oil emulsions encountered in bitumen and crude oil production.

AUTHOR INFORMATION

Corresponding Author

*E-mail: hongbo.zeng@ualberta.ca (H.Z.); zhenghe.xu@ualberta.ca (Z.X.). Phone: 780-492-1044 (H.Z.); 780-492-7667 (Z.X.). Fax: 780-492-2881 (H.Z.); 780-492-2881 (Z.X.).

Author Contributions

[†]A. Natarajan and J. Xie contributed equally to this work.

ACKNOWLEDGMENT

H. Zeng thanks the support of an NSERC Discovery Grant Award. The authors acknowledge the NSERC Industrial Research Chair Program in Oil Sands Engineering for the support of the study. Thanks are due to Syncrude Canada Ltd. for providing the bitumen samples. The SFA and AFM used in this study were purchased under CFI funds which are greatly appreciated.

REFERENCES

- (1) Mitchell, D. L.; Speight, J. G. *Fuel* **1973**, *52*, 149–152.
- (2) Yen, T. F.; Erdman, J. G.; Pollack, S. S. *Anal. Chem.* **1961**, *33*, 1587–1594.
- (3) Speight, J. G. *Asphaltenes and Asphalts*, 1; Yen, T. F., Chilingarian, G. V., Eds.; Elsevier Science: Amsterdam, 1994, p 7.
- (4) Wu, X.; van de Ven, T. G. M.; Czarnecki, J. *Colloids Surf. A* **1999**, *149*, 577–583.
- (5) Sjöblom, J.; Urbahl, O.; Grete, K.; Børve, N.; Mingyuan, L.; Saeten, J. O.; Christy, A. A.; Gu, T. *Adv. Colloid Interface Sci.* **1992**, *41*, 241–271.
- (6) Sjöblom, J.; Mingyuan, L.; Christy, A. A.; Ronningsen, H. P. *Colloids Surf. A* **1995**, *96*, 261–272.
- (7) Yarranton, H. W.; Hussein, H.; Masliyah, J. H. *J. Colloid Interface Sci.* **2000**, *228*, 52–63.
- (8) Taylor, S. D.; Czarnecki, J.; Masliyah, J. *J. Colloid Interface Sci.* **2002**, *252*, 149–160.
- (9) Zhang, L. Y.; Xu, Z.; Masliyah, J. H. *Langmuir* **2003**, *19*, 9730–9741.
- (10) Wu, X. *Energy Fuels* **2003**, *17*, 179–190.
- (11) Spiecker, P. M.; Kilpatrick, P. K. *Langmuir* **2004**, *20*, 4022–4032.
- (12) Zhang, L. Y.; Xu, Z.; Masliyah, J. H. *Ind. Eng. Chem. Res.* **2005**, *44*, 1160–1174.
- (13) Abraham, T.; Christendat, D.; Karan, K.; Xu, Z.; Masliyah, J. *Ind. Eng. Chem. Res.* **2002**, *41*, 2170–2177.
- (14) Zhang, L. Y.; Lawrence, S.; Xu, Z.; Masliyah, J. H. *J. Colloid Interface Sci.* **2003**, *264*, 128–140.
- (15) Horva Szabo |, G.; Masliyah, J. H.; Elliott, J. A. W.; Yarranton, H. W.; Czarnecki, J. *J. Colloid Interface Sci.* **2005**, *283*, 5–17.
- (16) Friberg, S. E.; Yang, H. F.; Midttun, O.; Sjöblom, J.; Aikens, P. A. *Colloids Surf. A* **1998**, *136*, 43–49.
- (17) Yan, N. X.; Masliyah, J. H. *J. Colloid Interface Sci.* **1994**, *168*, 386–392.
- (18) Kilpatrick, P. K.; Spiecker, P. M. Asphaltene Emulsions. In *Encyclopaedic Handbook of Emulsion Technology*; Sjöblom, J., Ed.; Marcel Dekker: New York, 2001.
- (19) Sjöblom, J.; Johnsen, E. E.; Westvik, A.; Ese, M. H.; Djuve, J.; Auflund, I. H.; Kallevik, H. Demulsifiers in the oil industry. In *Encyclopaedic Handbook of Emulsion Technology*; Sjöblom, J., Ed.; Marcel Dekker: New York, 2001.
- (20) McLean, J. D.; Kilpatrick, P. K. *J. Colloid Interface Sci.* **1997**, *189*, 242–253.
- (21) Czarnecki, J.; Moran, K. *Energy Fuels* **2005**, *19*, 2074–2079.
- (22) Czarnecki, J. *Energy Fuels* **2009**, *23*, 1253–1257.
- (23) Yeung, A.; Dabros, T.; Czarnecki, J.; Masliyah, J. *Proc. R. Soc. London, Ser. A* **1999**, *455*, 3709–3723.
- (24) Tsamantakis, C.; Masliyah, J.; Yeung, A.; Gentzis, T. *J. Colloid Interface Sci.* **2005**, *284*, 176–183.
- (25) Zhang, L. Y.; Lawrence, S.; Xu, Z.; Masliyah, J. H. *J. Colloid Interface Sci.* **2003**, *264*, 128–140.
- (26) Zhang, L. Y.; Breen, P.; Xu, Z.; Masliyah, J. H. *Energy Fuels* **2007**, *21*, 274–285.
- (27) Nordgård, E. L.; Sørland, G.; Sjöblom, J. *Langmuir* **2010**, *26*, 2352–2360.
- (28) Aston, D. E.; Berg, J. C. *J. Pulp Pap. Sci.* **1998**, *24*, 121–125.
- (29) Hartley, P. G.; Grieser, F.; Mulvaney, P.; Stevens, G. W. *Langmuir* **1999**, *15*, 7282–7289.
- (30) Mulvaney, P.; Perera, J. M.; Biggs, S.; Grieser, F.; Stevens, G. W. *J. Colloid Interface Sci.* **1996**, *183*, 614–616.
- (31) Snyder, B. A.; Aston, D. E.; Berg, J. C. *Langmuir* **1997**, *13*, 590–593.
- (32) Drummond, C.; Israelachvili, J. *J. Pet. Sci. Eng.* **2004**, *45*, 61–81.
- (33) Wu, X.; Czarnecki, J.; Hamza, N.; Masliyah, J. *Langmuir* **1999**, *15*, 5244–5250.
- (34) Wu, X.; Dabros, T.; Czarnecki, J. *Langmuir* **1999**, *15*, 8706–8713.
- (35) Christenson, H. K.; Israelachvili, J. N. *J. Colloid Interface Sci.* **1987**, *119*, 194–202.
- (36) Liu, J. J.; Xu, Z. H.; Masliyah, J. *Langmuir* **2003**, *19*, 3911–3920.
- (37) Liu, J. J.; Xu, Z. H.; Masliyah, J. *AIChE J.* **2004**, *50*, 1917–1927.
- (38) Liu, J. J.; Xu, Z. H.; Masliyah, J. *Can. J. Chem. Eng.* **2004**, *82*, 655–666.
- (39) Liu, J. J.; Xu, Z. H.; Masliyah, J. *Colloids Surf., A* **2005**, *260*, 217–228.

- (40) Li, H.; Long, J.; Xu, Z.; Masliyah, J. H. *Energy Fuels* **2005**, *19*, 936–943.
- (41) Liu, J. J.; Zhang, L. Y.; Xu, Z. H.; Masliyah, J. *Langmuir* **2006**, *22*, 1485–1492.
- (42) Wang, S.; Liu, J.; Zhang, L.; Xu, Z.; Masliyah, J. *Energy Fuels* **2009**, *23*, 862–869.
- (43) Wang, S.; Liu, J.; Zhang, L.; Xu, Z.; Masliyah, J. *Langmuir* **2010**, *26*, 183–190.
- (44) Vuillaume, K.; Giasson, S. *J. Phys. Chem. C* **2009**, *113*, 3660–3665.
- (45) Israelachvili, J.; Min, Y.; Akbulut, M.; Alig, A.; Carver, G.; Greene, W.; Kristiansen, K.; Meyer, E.; Pesika, N.; Rosenberg, k.; Zeng, H. *Rep. Prog. Phys.* **2010**, *73* (036601), 1–16.
- (46) Israelachvili, J. N. *Intermolecular and Surface Forces*, 2nd ed.; Academic Press: New York, 1991; p 291.
- (47) Akbulut, M.; Alig, A. R. G.; Min, Y.; Belman, N.; Reynolds, M.; Golan, Y.; Israelachvili, J. *Langmuir* **2007**, *23*, 3961–3969.
- (48) Israelachvili, J. N. *J. Colloid Interface Sci.* **1973**, *44*, 259–272.
- (49) Zeng, H.; Tian, Y.; Zhao, B.; Tirrell, M.; Israelachvili, J. *Macromolecules* **2007**, *40*, 8409–8422.
- (50) Degennes, P. G. *Adv. Colloid Interface Sci.* **1987**, *27*, 189–209.
- (51) Kuhl, T. L.; Leckband, D. E.; Lasic, D. D.; Israelachvili, J. N. *Biophys. J.* **1994**, *66*, 1479–1488.
- (52) Efremova, N. V.; Bondurant, B.; O'Brien, D. F.; Leckband, D. E. *Biochemistry* **2000**, *39*, 3441–3451.
- (53) Butt, H. J.; Kappl, M.; Mueller, H.; Raiteri, R.; Meyer, W.; Ruhe, J. *Langmuir* **1999**, *15*, 2559–2565.
- (54) Kamiyana, Y.; Israelachvili, J. *Macromolecules* **1992**, *25*, 5081–5088.
- (55) Mostowfi, F.; Indo, K.; Mullins, O. C.; McFarlane, R. *Energy Fuels* **2009**, *23*, 1194–1200.
- (56) Masliyah, J. H.; Bhattacharjee, S. *Electrokinetics and Colloid Transport Phenomena*; John Wiley & Sons: New York, 2006.
- (57) Fotland, P.; Askvik, K. M. *Colloids Surf. A* **2008**, *324*, 22–27.
- (58) Stachowiak, C.; Viguie, J. R.; Grolier, J. P. E.; Rogalski, M. *Langmuir* **2005**, *21*, 4824–4829.
- (59) Takanohashi, T.; Sato, S.; Saito, I.; Tanaka, R. *Energy Fuels* **2003**, *17*, 135–139.
- (60) Anderson, T. H.; Donaldson, S. H.; Zeng, H.; Israelachvili, J. N. *Langmuir* **2010**, *26*, 14458–14465.
- (61) Hwang, D. S.; Zeng, H.; Masic, A.; Harrington, M. J.; Israelachvili, J. N.; Waite, J. H. *J. Biol. Chem.* **2010**, *285*, 25850–25858.
- (62) Hwang, D. S.; Zeng, H.; Srivastava, A.; Krogstad, D. V.; Tirrell, M.; Israelachvili, J. N.; Waite, J. H. *Soft Matter* **2010**, *6*, 3232–3236.
- (63) Zeng, H.; Hwang, D. S.; Israelachvili, J. N.; Waite, J. H. *Proc. Natl. Acad. Sci. U.S.A.* **2010**, *107*, 12850–12853.
- (64) Blomberg, E.; Claesson, P. M.; Warnheim, T. *Colloids Surf. A* **1999**, *159*, 149–157.